University of Sistan and Baluchestan

Chemical Process Design

Available online at http://cpd.usb.ac.ir/

Elucidating Adsorption Mechanisms of Copper Ions on Surfactant-Modified Zeolites: An Integrated Study of Isotherm Modeling and Surface Characterization

Razieh Kazemi[1], Abbas kasaei[2]✉

[1] Department of Chemistry, Do.C., Islamic Azad University, Doroud, Iran. Email: raziehkazemi300@gmail.com
[2] Corresponding Author, Department of Chemistry, Do.C., Islamic Azad University, Doroud, Iran. Email: ab.kasaei1354@iau.ac.ir

ARTICLE INFO

Article type:
Research Article

Article history:
Received: 2025-08-17
Received in revised form: 2026-02-10
Accepted: 2026-02-12
Available online: 2026-02-12

Keywords: *Zeolite; Surfactant modification; Copper adsorption; Adsorption mechanism; Isotherm modeling*

ABSTRACT

This research examines the adsorption mechanisms pertaining to copper ions on clinoptilolite zeolite that has been modified with cationic (CTAB) and anionic (SDS) surfactants. Given that the fundamental principles that dictate adsorption phenomena, particularly the influence of surfactant charge, are not thoroughly comprehended, this investigation adopts a comprehensive methodology that integrates isotherm modeling alongside surface characterization data to scrutinize the adsorption dynamics. Equilibrium data were subjected to analysis through a variety of isotherm models. The findings indicated that the SDS-modified zeolite demonstrated a significantly enhanced adsorption capacity (19.56mg/g), which is more than twice that of the unmodified zeolite (8.98mg/g). The adsorption behavior was most accurately represented by the Redlich-Peterson isotherm, with the observed performance improvement ascribed to the synergistic effects resulting from an increased specific surface area and favorable electrostatic interactions. In contrast, zeolite modified with CTAB exhibited a diminished adsorption capacity of 7.08mg/g, while the Frumkin isotherm suggested the presence of repulsive interactions. For the unaltered zeolite, the Weber-van Vliet model yielded the most accurate representation, indicating a hybrid mechanism of adsorption. This research underscores the notion that the charge of the surfactant is a pivotal determinant of the adsorption mechanism. By disentangling the influences of surface area from electrostatic interactions, it establishes a quantitative framework for the development of effective adsorbents.

Cite this article: Kazemi, R., Kasaei, A., (2026), Elucidating Adsorption Mechanisms of Copper Ions on Surfactant-Modified Zeolites: An Integrated Study of Isotherm Modeling and Surface Characterization, *Chemical Process Design*, 5(2), 00-00. http//doi.org/10.22111/cpd.2026.52973.1073

DOI: http//doi.org/10.22111/cpd.2026.52973.1073

Publisher: University of Sistan and Baluchestan.

1. Introduction

Heavy metals are defined as elements exhibiting significant atomic mass or elevated density (exceeding 5g/cm³) [1]. The designation "heavy metals" encompasses both metallic and metalloid elements that pose toxicity risks to ecological systems. The escalating levels of heavy metals in the environment may be attributed to either natural or anthropogenic sources. Natural sources encompass processes such as rock weathering and volcanic eruptions, whereas predominant anthropogenic sources comprise industrial operations including electroplating, battery fabrication, pesticide synthesis, mining activities, rayon production, metal washing procedures, leather processing, fluidized bed bioreactors, textile fabrication, metal smelting, petrochemical manufacturing, paper production, and electrolysis techniques [2]. With the proliferation of industrial activities and anthropogenic endeavors, the prevalence of heavy metals in wastewater is experiencing an upward trajectory. Contaminated wastewater ultimately infiltrates the environment, posing significant risks to both human health and ecological systems. Heavy metals are characterized by their non-biodegradable nature [3] and have been linked to severe health complications, including malignancies of the skin, liver, lungs, and bladder, as well as damage to cerebral and reproductive organs, renal dysfunction, and disorders of the immune system [4–12].

The heavy metals that are most frequently encountered encompass lead (Pb), zinc (Zn), mercury (Hg), nickel (Ni), cadmium (Cd), copper (Cu), chromium (Cr), and arsenic (As). Although these metals may be present in trace concentrations, they nonetheless present considerable hazards. Copper, in particular, is a heavy metal that is extensively utilized across various applications. It may enter the environment due to mining operations or through the utilization of copper-containing items such as batteries, mobile devices, plumbing systems, semiconductors, or from natural sources. While copper is essential for the metabolic processes in both humans and animals, elevated concentrations in the environment pose a significant threat to public health. Prolonged exposure to copper via contaminated water sources may result in critical toxicological consequences including emesis, myalgia, and convulsions [13]. The United States Environmental Protection Agency (USEPA) categorizes copper as a priority pollutant owing to its enduring and irreversible toxicological properties [14].

Recent scholarly investigations have concentrated on a multitude of methodologies aimed at the extraction of heavy metal ions, encompassing electrocoagulation (EC), adsorption utilizing both natural and synthetic adsorbents, the utilization of magnetic fields, advanced oxidation techniques, membrane technologies, among other approaches [15,16]. Within this spectrum, adsorption emerges as one of the most prevalently employed techniques. The mechanism of adsorption is modulated by the physicochemical characteristics of both the adsorbent and the metal ions, in conjunction with operational parameters such as temperature, adsorbent dosage, pH level, contact duration, and initial ion concentration. In general, heavy metal ions are capable of being adsorbed onto the surfaces of adsorbent materials. This research endeavors to examine the adsorption characteristics of copper ions utilizing natural clinoptilolite zeolite, alongside its modified variants, for the purposes of separation and extraction.

Natural zeolites are hydrated aluminosilicate minerals characterized by a porous framework and exhibit physicochemical properties, including cation exchange, molecular sieving, catalysis, and adsorption. The utilization of natural zeolites for environmental applications has recently garnered substantial scholarly interest, predominantly attributable to their distinctive properties and widespread availability across the globe. Their utilization in the treatment of water and wastewater has been extensively investigated and continues to represent a promising strategy in environmental remediation endeavors. In the last few decades, natural zeolites have been predominantly employed

for the elimination of ammonium, heavy metals, and organic compounds due to their inherent ion-exchange capabilities [17–25]. Zeolites possess the ability to engage in ion exchange with their surrounding milieu—this represents one of their most critical attributes. The ion-exchange dynamics of natural zeolites are influenced by various factors, such as the structural configuration of the framework, the dimensions and morphology of the ions, the charge density of the anionic framework, and the concentration of external electrolyte solutions [26,27].

In recent decades, a plethora of scholarly investigations have concentrated on the modification of natural zeolites with the aim of augmenting their specific surface area or enhancing selectivity towards specific substances. Prevalent modification techniques encompass thermal activation (either in a single-step or combined approach), chemical treatment (utilizing acids, bases, or inorganic salts), surfactant modification, and treatment with metal oxides. When selecting an appropriate modification technique, it is imperative to consider both the intended application and the economic viability thereof [28]. A particularly prevalent method for altering surface characteristics is the utilization of organic surfactants. Surfactants including tetramethylammonium [29,30], cetyltrimethylammonium (CTMA) [31,32], hexadecyltrimethylammonium (HDTMA) [29,33–38], octadecyldimethylbenzylammonium (ODMBA) [31,39–41], n-cetylpyridinium (CPD) [42], benzyltetradecylammonium (BDTDA) [38], stearyldimethylbenzylammonium (SDBAC) [43–45], N,N,N-, and polyhexamethylene-guanidine [46] have been employed for the modification of zeolites.

In recent years, there has been a notable increase in the documentation of both natural zeolites and their modified variants being utilized for the separation and removal of anions, organic compounds, and heavy metals from aqueous environments.

Bagheri et al. examined the elimination of Sunset Yellow (E110) utilizing natural zeolite and zeolite altered with the cationic surfactant cetylpyridinium chloride (CPC) through the adsorption technique. The outcomes demonstrated that the surfactant-modified zeolite (SMZ) displayed a superior adsorption capacity for Sunset Yellow in comparison to the unmodified (natural) zeolite. The empirical adsorption data were scrutinized nonlinearly employing isotherm equations such as Langmuir, Freundlich, Tempkin, Langmuir-Freundlich (also referred to as Sips), and Extended Langmuir (EL). The empirical data revealed a more favorable fit with the Sips isotherm. Maximum dye elimination transpired in less than 5 minutes, and the utmost adsorption capacity was 5.06mg per gram. The conclusions of this investigation imply that surfactant-modified cationic zeolite is an efficacious adsorbent for the extraction of anionic dyes from aqueous solutions [47].

Kaolin modified with cetyl trimethyl ammonium (CTAB) eliminates both Cu(II) and organic contaminants, such as o-xylene and phenol. The modification significantly enhances the adsorption capability of the natural kaolin (19.2 and 5.1mg/g for Cu(II) and phenol, respectively) up to 38.5mg/g for Cu(II), 91.5mg/g for phenol, and 51.8mg/g for o-xylene. The utilization of the zwitterionic surfactant hexadecyldimethyl (3-sulphonatopropyl) ammonium on montmorillonite facilitates the removal of Cu(II) and phenol; however, the comparison with HDTMA-Br montmorillonite indicates that the adsorption capability of the clay, both for organics and metals, is marginally superior when employing a cationic surfactant. Nevertheless, the introduction of quaternary ammonium cations on montmorillonites diminished the metal adsorption capability of the clay since the interlayer quaternary ammonium cations are not readily exchangeable or the hydrophobic interlayer milieu of the montmorillonite constrains the adsorption towards the hydrated metal cation [48].

Natural zeolite sourced from the Nourkough Mine in Armenia underwent modification employing the anionic surfactant sodium dodecyl sulfate (SDS) in conjunction with the cationic surfactant cetyl trimethyl ammonium bromide (CTAB). The resulting modified samples were subsequently utilized for the extraction of metallic ions from aqueous environments. The data presented substantiate that the surfactant-modified natural zeolites derived from the Nor Koghb deposit (Noyemberyan, Armenia) serve as efficacious adsorbents for the elimination of metal ions from aqueous media, applicable in both single-component and multi-component adsorption scenarios. It was determined that, in the context of single-component adsorption, the adsorption efficacy on anionic surfactant-modified zeolite (SMZ) follows the hierarchy $CO_2^+ > Fe^{2+} > Ni^{2+} > Cu^{2+} > Zn^{2+} > Mn^{2+} > Pb^{2+}$, with the adsorption process being more accurately characterized by the Freundlich isotherm, indicating a multilayer adsorption phenomenon. Furthermore, it was demonstrated that for chromium in the hexavalent state (Cr(VI)), the cationic SMZ proves to be a highly effective adsorbent, enhancing the adsorption of Cr(VI) by approximately five-fold relative to natural zeolite. Investigations into the textural and surface characteristics of SMZ revealed a significant increase in specific surface area and microporosity as a result of the modification process, which, undoubtedly, augments the adsorption capacity of the modified samples. Fourier-transform infrared (FTIR) analyses confirmed the establishment of an external surface layer induced by surfactants, alongside an increase in the quantity of charged sites (both positive and/or negative) on the zeolite surface as a consequence of modification, which is crucial for determining the adsorption efficiency concerning metal ions in aqueous environments [49].

Majidi et al. conducted a modification of natural clinoptilolite zeolite utilizing the cationic surfactant cetyltrimethylammonium bromide (CTAB) and subsequently employed this modified zeolite as an adsorbent for the extraction of volatile organic compounds (VOCs) from kerosene. The optimization of adsorption efficiency (R%) was systematically approached through experimental design methodologies. Factors such as contact time, pH level, and adsorbent dosage, which may significantly impact the adsorption efficiency, were meticulously evaluated during the optimization procedure. The outcomes of the optimization process revealed that the peak adsorption efficiency was attained at a pH of 3.0, an adsorbent dosage of 0.4g, and a contact duration of 180 minutes. In order to elucidate the adsorption characteristics, both the Freundlich and Langmuir isotherm models were rigorously analyzed. Furthermore, the thermodynamic assessment indicated that the process was both spontaneous and endothermic in nature. The findings elucidated that the adsorption mechanism conformed to the Langmuir isotherm model, exhibiting a coefficient of determination (R^2) of 0.9906. The adsorption efficiency of volatile organic compounds (VOCs) from kerosene utilizing surfactant-modified zeolite was markedly improved. This investigation underscores the efficacy of surfactant-modified clinoptilolite as a viable and commendable adsorbent for the reduction of VOC emissions originating from kerosene, thereby facilitating the advancement of more sustainable environmental practices [50].

Shirendev et al. conducted an investigation into the removal of copper (II) ions from aqueous solutions utilizing zeolite that had been modified with the silicon monomer (3-aminopropyltriethoxysilane; APTES), with outcomes influenced by pH levels, duration, temperature, and the initial concentration of Cu(II) ions. The peak adsorption capacity of the modified zeolite for Cu(II) was ascertained to be 4.50, 6.244, 6.96, and 20.66 mg/g at a temperature of 25°C (pH = 5, duration = 8 hours), corresponding to the initial Cu(II) concentrations of 50, 100, 200, and 400 mg/L, respectively. According to the principles governing adsorption thermodynamics and kinetics, the adsorption process is predominantly regulated by a second-order reaction. Utilizing two established isotherm models (Langmuir and Freundlich) characterized by constant parameters (KL=0.144, n=2.764) and correlation coefficients (R^2=0.8946,

R^2=0.9216), it was deduced that the adsorption of copper (II) onto the modified zeolite is more accurately represented by the Freundlich isotherm model as opposed to the Langmuir isotherm model. The modified zeolite demonstrates potential as an efficacious material for the extraction of copper (II) from aqueous solutions [51].

Roshan Zekavat et al. employed hexadecyltrimethylammonium bromide (HDTMA-Br) modified clinoptilolite for the concurrent elimination of copper and hexavalent chromium from aqueous environments. The Langmuir isotherm model exhibited the most accurate representation of the equilibrium data for Cu^{2+} and Cr(VI), resulting in maximum adsorption capacities of 0.068 and 0.0093mmol/g, respectively. The mechanism of sorption was identified as being governed by intra-particle diffusion processes. The results demonstrated that the surfactant modification induces a transformation of the zeolite's surface charge from negative to positive, thereby converting it into a cost-effective adsorbent adept at the simultaneous extraction of both cations and oxyanions. Moreover, the study uncovered that the efficacy of Cr(VI) removal is significantly augmented in the presence of copper cations, which can be attributed to the increased availability of positive surface sites on the adsorbent [52].

Oter and Akcay conducted a comprehensive investigation into a Turkish natural clinoptilolite for the purpose of assessing its efficacy in the adsorption of Pb^{2+}, Ni^{2+}, Cu^{2+}, and Zn^{2+} ions from both single-ion and mixed-ion solutions. Various parameters, including contact time, initial pH, solid-to-liquid ratio, and initial metal ion concentration, were systematically evaluated. The maximum adsorption capacities were ascertained to be 0.730, 0.251, and 0.173meq/g for Pb^{2+}, Zn^{2+}, and Cu^{2+}, respectively, while comparatively lower values were recorded for mixed-ion solutions, specifically 0.299, 0.108, 0.022, and 0.017meq/g for Pb^{2+}, Zn^{2+}, Cu^{2+}, and Ni^{2+}, respectively [53].

A naturally occurring clinoptilolite was transformed into a clinoptilolite–iron oxide (Clin–Fe) composite for the purpose of removing Mn^{2+} [54], Zn^{2+} [55], and Cu^{2+} [56] from potable water samples. Under controlled laboratory conditions, the peak adsorption capacity for Mn was determined to be 7.69mg/g for the unmodified clinoptilolite and 27.1mg/g for the Clin–Fe composite. Regarding Zn, the adsorption capacities recorded were 71.3mg/g and 94.8mg/g, while for Cu, the respective values were 13.6mg/g and 37.5mg/g. These findings elucidate the enhanced metal adsorption capabilities attributable to the augmentation of ion-exchange processes.

This study seeks to respond to the following research gaps:

- How does surface modification of natural clinoptilolite zeolite with anionic (SDS) and cationic (CTAB) surfactants affect its adsorption capacity and efficiency for copper cations (Cu^{2+}) in aqueous solution?
- What is the mechanistic role of surfactant charge (anionic vs. cationic) in altering the surface properties of zeolite and its subsequent affinity for cationic copper pollutants?
- Which adsorption isotherm models most accurately describe the equilibrium data for copper adsorption onto natural, CTAB-modified, and SDS-modified zeolites?

The fundamental aim of the present investigation is not the refinement of operational parameters; instead, it seeks to furnish a comprehensive and mechanistic elucidation of how the positive charge of the surfactant in cetyltrimethylammonium bromide (CTAB) and the negative charge in sodium dodecyl sulfate (SDS) affect the adsorption isotherm, thermodynamic properties, and the intrinsic mechanism that governs the adsorption of copper ions. To realize this objective, a holistic methodology that integrates advanced isotherm modeling alongside surface characterization techniques has been utilized.

2. Methods

In order to formulate copper solutions, a stock solution exhibiting a concentration of 200mg/L (ppm) was meticulously synthesized by dissolving copper sulfate in deionized water. From this stock solution, additional solutions with the following concentrations were subsequently prepared through dilution to a final volume of 50mL: 200, 180, 160, 150, 140, 120, 100, 80, 60, 50, 40, 20, and 10 ppm. The absorbance of these solutions was quantified utilizing an atomic absorption spectrophotometer, and a calibration curve was constructed in accordance with the absorbance measurements (Fig. 1).

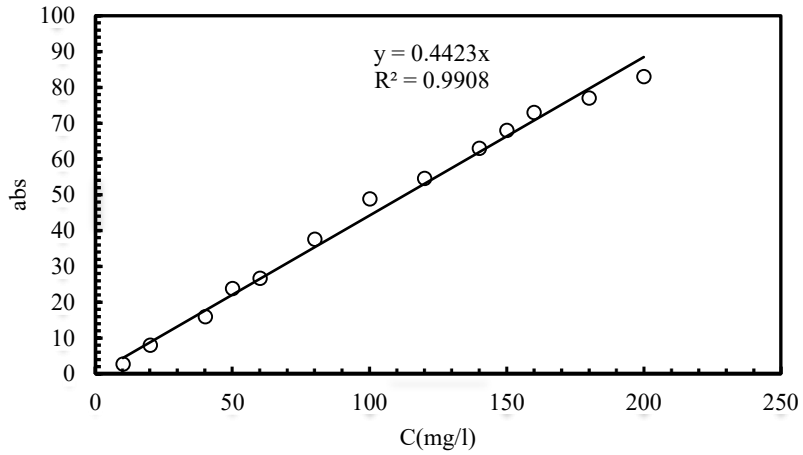

Fig. 1. Calibration curve of absorbance values quantified by atomic absorption spectroscopy for copper solutions of varying concentrations

In order to examine the adsorption characteristics of copper ions onto unmodified natural clinoptilolite zeolite, aqueous solutions of copper with volumes of 100mL and concentrations of 200, 180, 160, 150, 140, 120, 100, 80, 60, 50, 40, 20, and 10mg/L (ppm) were meticulously prepared. A precise mass of one gram of natural clinoptilolite zeolite was incorporated into each individual solution, and the Erlenmeyer flasks were subsequently sealed with Parafilm to prevent any external contamination. The resulting samples, in conjunction with a control solution consisting of only the water solvent and one gram of zeolite, were subjected to agitation for a duration of one hour using a mechanical shaker. Following the attainment of equilibrium concerning the concentration of the adsorbate, the samples underwent filtration through filter paper and were subsequently centrifuged at a speed of 13,000rpm for a period of 20 minutes. The quantification of the adsorption process was subsequently performed utilizing Atomic Absorption Spectroscopy (AAS).

For the purpose of surface modification of the natural clinoptilolite zeolite, the zeolites underwent an initial washing process utilizing boiling distilled water. Subsequently, they were subjected to thermal treatment in an oven set at 80°C for a duration of 1 hour, aimed at the removal of any surface contaminants as well as the expulsion of water from both the zeolite's structural framework and internal voids. Aqueous solutions containing the cationic surfactant hexadecyltrimethylammonium bromide (CTAB) and the anionic surfactant sodium dodecyl sulfate (SDS) were formulated at a concentration of 0.5M. For every 100mL of surfactant solution prepared, 5grams of the washed zeolite was systematically incorporated into the mixture. The Erlenmeyer flasks were subsequently sealed with Parafilm and agitated for a period of 24 hours at a rotational speed of 180rpm. Following this procedure, the zeolites were filtered using filter paper and subsequently dried in an oven maintained at 80°C for 2 hours. Scanning Electron Microscope (SEM) imagery illustrating both the natural zeolite and the zeolites modified with CTAB and SDS is provided in Fig.

2. The Fourier Transform Infrared (FT-IR) spectra pertaining to the natural zeolite, cetyltrimethylammonium bromide (CTAB), sodium dodecyl sulfate (SDS), as well as zeolites that have undergone modification with CTAB and SDS, are illustrated in Fig. 3.

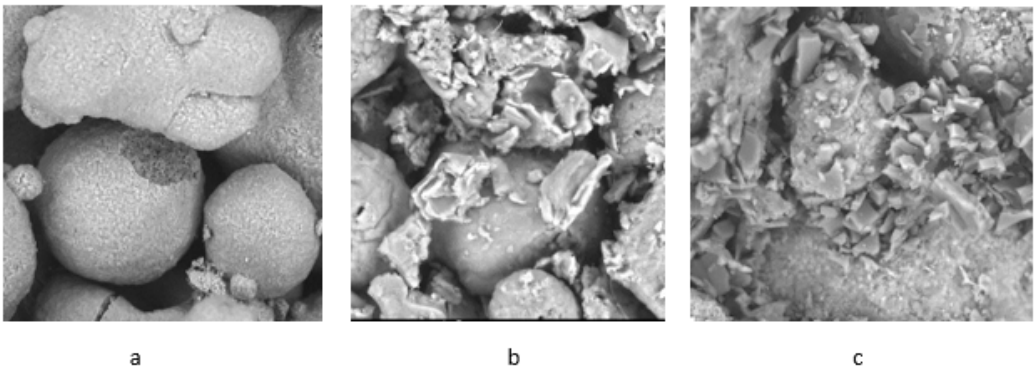

Fig. 2. Scanning Electron Microscope (SEM) images of natural zeolite (a) and zeolites modified with surfactants SDS (b) and CTAB (c)

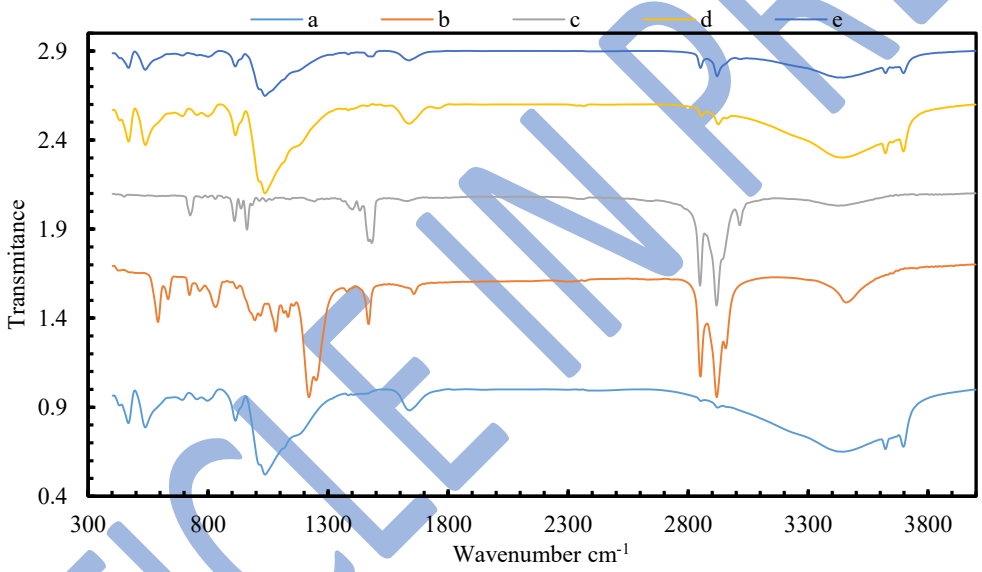

Fig. 3. FT-IR spectra of natural zeolite (a), SDS (b), CTAB (c), and zeolites modified with SDS (d) and CTAB (e)

2.1. Interpretation of FT-IR spectra for natural and surfactant-modified zeolites (CTAB and SDS)

2.1.1. Raw zeolite

The FT-IR spectrum of raw zeolite indicates the presence of characteristic groups confirming the silicate skeletal structure of the zeolite:

- The stretching bands of Si–O–Si and Si–O–Al are clearly observed in the 1000–1100cm^{-1} region.
- A broad absorption band at 3400–3600cm^{-1} corresponds to the stretching vibrations of O–H groups (physically adsorbed water or hydroxyl groups).
- A band at 1630–1650cm^{-1} is attributed to bending vibrations of adsorbed water.

2.1.2. SDS surfactant

The FT-IR spectrum of SDS, an anionic surfactant, shows distinctive bands:

- Stretching bands at 2920 and 2850 cm^{-1} corresponding to alkyl CH_2 and CH_3 groups.

- A strong band at 1220–1240cm^{-1} and subsidiary bands around 1050cm^{-1} related to the stretching vibrations of sulfate groups S=O and S–O.
- Weaker bands in the 800–1000cm^{-1} region related to the hydrocarbon skeleton structure.

2.1.3. CTAB surfactant:

The FT-IR spectrum of CTAB, a cationic ammonium surfactant, is characterized by:

- C–H stretching bands at 2920 and 2850cm^{-1} similar to SDS.
- CH_2 bending bands around 1460cm^{-1}.
- Absence of sulfate-related bands distinguishes it from SDS.

2.1.4. SDS-modified zeolite:

The FT-IR spectrum of SDS-modified zeolite shows a combination of characteristic bands of both zeolite and SDS:

- Zeolitic Si–O–Al and Si–O–Si bands are preserved.
- Clear alkyl C–H bands at 2920 and 2850cm^{-1} indicate surface coating of zeolite with SDS.
- The S=O band near 1220cm^{-1} confirms sulfate groups are stabilized on the zeolite surface.
- A shift in the O–H band around 3400cm^{-1} suggests hydrogen bonding interactions between the zeolite surface groups and SDS.

2.1.5. CTAB-modified zeolite

This sample exhibits combined features of zeolite and CTAB:

- Distinct C–H stretching bands at 2920 and 2850cm^{-1}.
- Preservation of zeolitic silicate bands in the 1000–1100cm^{-1} range.
- A broadened and shifted O–H band near 3400cm^{-1}, possibly due to adsorption of ammonium groups of CTAB on the zeolite surface.

Overall, the FT-IR spectra and SEM images demonstrate the successful surface modification of zeolite with SDS and CTAB surfactants. The presence of characteristic surfactant bands on modified zeolite spectra, along with shifts in O–H bands and increased alkyl bands, confirms the stabilization of surfactant molecules on the zeolite surface. This significantly enhances the surface properties of zeolite and its applicability in adsorption processes.

With reference to the BET analytical findings documented in the scholarly literature [49] concerning both unaltered zeolite and zeolites subjected to modification through the incorporation of SDS and CTAB surfactants, it can be discerned that there is a notable enhancement in the specific surface area, external surface area, mesopore volume, micropore volume, and micropore surface area as a consequence of the aforementioned modifications (Table 1).

Table 1. Values of characteristic parameters of natural and SM zeolites*

Type of zeolite	Sspecific, m^2/g	Sexternal, m^2/g	Smicro, m^2/g	Vmeso, cm^3/g	Vmicro, cm^3/g
Natural zeolite	19.40	15.57	3.98	1.44	4.03
SDS-modified zeolite	72.70	18.00	54.70	3.54	17.90
CTAB-modified zeolite	93.60	25.40	68.20	5.24	29.81

* – Note: Estimated uncertainties are ±0.20 m^2/g for Sspecific, ±0.20 m^2/g for Sexternal, ±0.20 m^2/g for Smicro, ±0.20 cm^3/g for Vmeso, and ±0.20 cm^3/g for Vmicro

Following the described procedure for raw zeolite, the adsorption of modified zeolites with CTAB and SDS surfactants on the sample solutions was measured by atomic absorption spectroscopy.

3. Results

Employing the absorbance values obtained for the solutions alongside the established calibration curve for anthracene (Fig. 1) and Eq. (1).

$$Y = 0.4423X \quad (1)$$

The equilibrium concentrations (C_e) were determined. Thereafter, utilizing the calculated C_e values, the initial concentration (C_0), the volume of the pollutant solution measured in liters (V), and the mass of the adsorbent (m), the amount of adsorbate per unit mass of adsorbent (q_e) was computed utilizing the following formula:

$$q_e = \frac{(c_0 - c_e)V}{m} \quad (2)$$

where:

q_e = Quantity of adsorbate per unit mass of adsorbent (mg/g)

C_0 = Initial concentration of the pollutant (mg/L or ppm)

C_e = Equilibrium concentration subsequent to adsorption (mg/L or ppm)

V = Volume of solution (L)

m = Mass of adsorbent (g)

Through a comparative analysis of the data acquired from the adsorption of copper onto natural zeolite, zeolite modified with the cationic surfactant cetyltrimethylammonium bromide (CTAB), and zeolite modified with the anionic surfactant sodium dodecyl sulfate (SDS), and by examining the equilibrium adsorption quantity (q_e) in each scenario, it was determined that the surface modification of zeolite utilizing the anionic surfactant SDS yielded the most pronounced performance and efficiency. For instance, in the case of a 200mg/L solution, the q_e value (19.56mg/g) was more than double that of the natural zeolite (q_e = 8.98mg/g). Conversely, the modification with the cationic surfactant CTAB not only failed to enhance the adsorption efficiency (q_e= 7.08mg/g) but also resulted in a decline in adsorption performance relative to the unmodified zeolite. This adsorption behavior is governed by electrostatic interactions between the surfactant-modified zeolite surface and copper(II) cations (Cu^{2+}).

When sodium dodecyl sulfate (SDS), an anionic surfactant, is employed, the negatively charged sulfate head groups (SO_4^-) adsorb onto the zeolite surface through physisorption mechanisms. This modification creates a negatively charged surface layer that exhibits strong electrostatic attraction toward Cu^{2+} ions, consequently enhancing both adsorption affinity and capacity.In contrast, modification with cetyltrimethylammonium bromide (CTAB), a cationic surfactant, and results in the formation of a positively charged surface layer due to the adsorption of quaternary ammonium head groups. The resulting positively charged surface generates electrostatic repulsion with Cu^{2+} ions, thereby hindering their approach to binding sites and significantly reducing both adsorption affinity and overall removal efficiency. Upon calculating q_e for each concentration, the q_e vs. C_e curve was subsequently plotted (Figs. 4–6).

The morphology of the aforementioned curves, alongside their juxtaposition with adsorption isotherms, suggests that the adsorption dynamics within the copper–natural clinoptilolite zeolite and surfactant-modified zeolite frameworks (specifically those modified with CTAB and SDS) adhere to a monolayer adsorption paradigm. Consequently, the empirical findings are amenable to fitting through monolayer adsorption isotherm models, including but not limited to Langmuir, Freundlich, Sips, Tempkin, and Reich-peterson, among others.

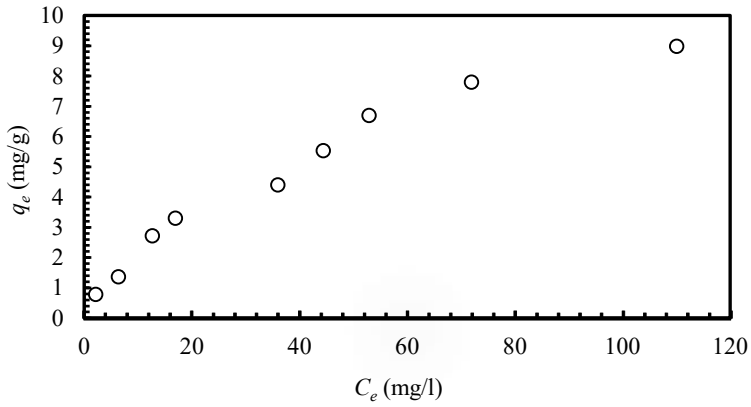

Fig. 4. Variation graph of q_e against C_e for the adsorption of copper on unmodified zeolite

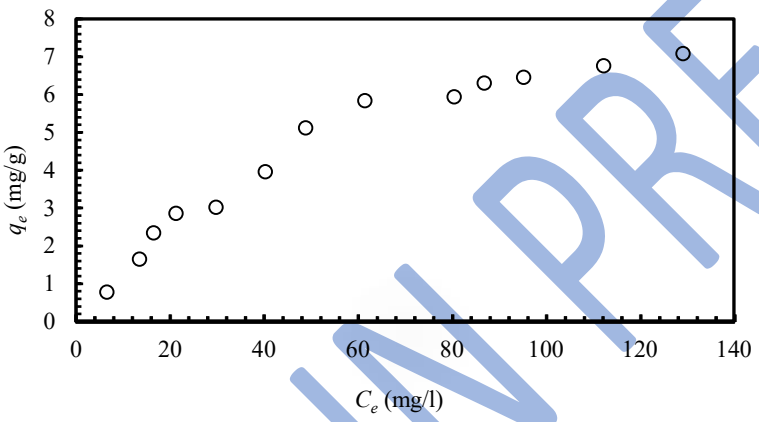

Fig. 5. Variation graph of q_e against C_e for the adsorption of copper on CTAB-modified zeolite

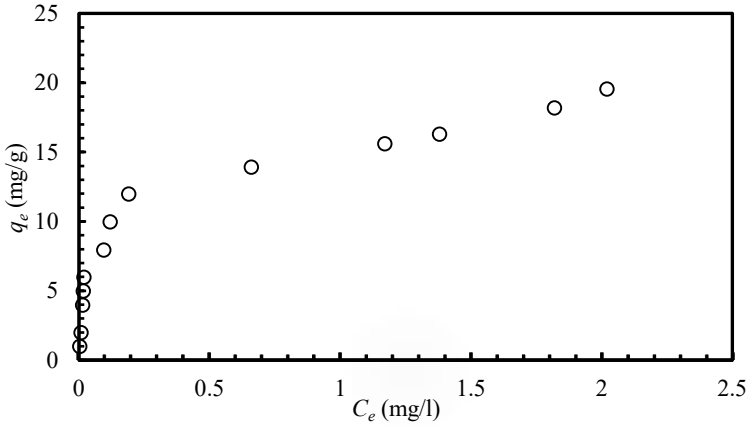

Fig. 6. Variation graph of q_e against C_e for the adsorption of copper on SDS-modified zeolite

In this context, the nonlinear formulations of these isotherms [57] were scrutinized, and the parameters associated with the isotherms were derived by fitting the empirical data with the aid of Curve Expert software. The outcomes of these fittings are encapsulated in Tables 2-6.

Table 2. Parameters and correlation coefficients (R) pertinent to nonlinear two-parameter adsorption isotherms derived from the fitting of experimental data via Curve Expert software for the adsorption of copper on both natural (unmodified) zeolite and zeolites that have been modified with CTAB and SDS

Isotherm	Isotherm equation	Unmodified natural zeolite			CTAB-modified zeolite			SDS-modified zeolite		
Langmuir	$q_e = \frac{q_m.b.c_e}{1+bc_e}$	q_m	b	R	q_m	b	R	q_m	b	R
		14.1449	0.0158	0.9915	10.7385	0.0159	0.9917	17.5969	13.1547	0.9698
Freundlich		k_f	n	R	k_f	n	R	k_f	n	R

	$q_e = k_f.C_e^{(\frac{1}{n})}$	0.5986	1/7053	0.9909	0.4976	1.7808	0.9781	15.6207	3.5241	0.9816
Tempkin	$q_e = B_T.\ln(A_T.c_e)$	B_T	A_T	R	B_T	A_T	R	B_T	A_T	R
		1.9606	0.4049	0.9214	2.2859	0.1705	0.9874	2.7092	355.3708	0.9888
Dubinin-Radushkevich	$q_e = q_s.\exp(-k_{ad} \times \varepsilon^2)$ $(\varepsilon = RT \times \ln(1+1/c_e))$	q_s	K_{ad}	R	q_s	K_{ad}	R	q_s	K_{ad}	R
		7.4346	243.3916	0.9126	6.4721	408.5693	0.9488	16.9744	0.0878	0.9735
Jovanovich	$q_e = q_m.(1-e^{-b.c_e})$	q_m	b	R	q_m	b	R	q_m	b	R
		10.0815	0.0197	0.9899	7.6209	0.0201	0.9933	16.5560	8.4855	0.9476
Elovich	$c_e = \frac{q_e}{q_m.K_E.\exp\left(\frac{-q_e}{q_m}\right)}$	q_m	K_E	R	q_m	K_E	R	q_m	K_E	R
		7.4727	0.0378	0.9916	4.3181	0.0691	0.9862	6.9297	21.4408	0.9816
Volmer	$c_e = \frac{q_e}{b(q_m-q_e)}.e^{\frac{q_e}{(q_m-q_e)}}$	b	q_m	R	b	q_m	R	b	q_m	R
		24.4011	0.0067	0.9930	16.0497	0.0137	0.9904	37.0772	1.9354	0.9717

Table 3. Parameters and correlation coefficients (R) associated with nonlinear three-parameter adsorption isotherms established through the fitting of experimental data employing Curve Expert software for the adsorption of copper on natural (unmodified) zeolite

Isotherm	Isotherm equation	Unmodified natural zeolite			
Reich-Peterson	$q_e = \frac{k_R.c_e}{1+a_R.c_e^g}$	k_R	a_R	g	R
		0.3522	0.1328	0.6783	0.9929
Sips	$q_e = \frac{k_s.a_s.c_e^{B_S}}{1+a_s.c_e^{B_s}}$	k_s	a_S	B_s	R
		21.3704	0.0179	0.7946	0.9935
Hill	$q_e = \frac{q_m.c_e^{n_H}}{K_D+c_e^{n_H}}$	q_m	n_H	K_D	R
		21.3703	0.7946	55.8362	0.9933
Toth	$q_e = \frac{k_T.c_e}{\left(a_T+c_e^z\right)^{\frac{1}{z}}}$	k_T	a_T	z	R
		36.7653	7.6677	0.4582	0.9931
Khan	$q_e = \frac{q_s.b_k.c_e}{(1+b_k.c_e)^{a_k}}$	q_s	b_k	a_k	R
		3.7762	0.0795	0.5617	0.9927
Radke-Prausnitz	$q_e = \frac{a_{RP}.r_{RP}.c_e}{1+r_{RP}.C_e^{B_{RP}}}$	a_{RP}	r_{RP}	B_{RP}	R
		2.6528	0.1327	0.6783	0.9929
Koble-Corrigan	$q_e = \frac{A.c_e^n}{1+B.C_e^m}$	A	n	B	R
		0.3827	0.7946	0.0179	0.9933
Keller	$q_e = \frac{q_m.a.b.c_e}{\left(1+(b.C_e)^a\right)^{1/a}}$	q_m	a	b	R
		80.2207	0.4582	0.0117	0.9931
Dobinin-Astakhov	$q_e = q_m.\exp\left(-\left(\frac{RT}{E}\ln\left(1+\frac{1}{c_e}\right)\right)^n\right)$	q_m	E	n	R
		132.7329	2.3313×10^4	0.1834	0.9930
Unilan	$q_e = \frac{q_m}{2s}.\ln\left(\frac{1+b.e^s.c_e}{1+b.e^{-s}.c_e}\right)$	q_m	b	s	R
		0.4006	-4.3342	7.4818×10^{-4}	0.9925
Jossens	$c_e = \frac{q_e}{H}.e^{\left(F.q_e^P\right)}$	H	F	P	R
		0.0016	2.0000	20.0000	0.9851
Hill-Debuer	$c_e = \frac{q_e}{b.(q_m-q_e)}.e^{\left(\frac{q_e}{q_m-q_e}\right)}.e^{\left(\frac{-cq_e}{q_m}\right)}$	q_m	b	c	R
		18.1321	1.8204	0.0097	0.9941
Frumkin	$c_e = \frac{\theta}{K_{FF}}.\exp\left(\frac{-f.\theta}{1-\theta}\right)$ $\left(\theta = \left(\frac{q_e}{b}\right)\right)$	b	f	k_{FF}	R
		0.0640	0.7863	-0.2324	0.9429
Fowler-Guggenheim	$c_e = \frac{q_e}{k_{FG}.(q_m-q_e)}.\exp\left(\frac{2.q_e.w}{R.T.q_m}\right)$	q_m	k_{FG}	w	R
		161.8798	572.1656	2.9347×10^{-4}	0.9916
Kiselev	$C_e = \frac{1}{k_1}.\left(\frac{q_e}{q_m-q_e}\right)+\frac{1}{k_1k_n}\left(\frac{q_m}{q_m-q_e}\right)$	k_1	q_m	k_n	R
		0.0157	14.2761	2.136310^7	0.9936

Table 4. Parameters and correlation coefficients (R) relevant to nonlinear three-parameter adsorption isotherms obtained from the fitting of experimental data through Curve Expert software for copper adsorption on zeolite modified with CTAB

Isotherm	Isotherm equation	CTAB-modified natural zeolite			
Reich-Peterson	$q_e = \frac{k_R.c_e}{1+a_R.c_e^g}$	k_R	a_R	g	R
		0.1386	0.0018	1.3917	0.9936
Sips	$q_e = \frac{k_s.a_s.c_e^{B_S}}{1+a_s.c_e^{B_s}}$	k_s	a_S	B_s	R
		8.8201	1.2447	104.5834	0.9934
Hill	$q_e = \frac{q_m.c_e^{n_H}}{K_D+c_e^{n_H}}$	q_m	n_H	K_D	R
		0.6037	3.3312	5.7579×10^{3}	0.9934
Toth	$q_e = \frac{k_T.c_e}{\left(a_T+c_e^z\right)^{\frac{1}{z}}}$	k_T	a_T	Z	R
		7.9022	1.7376×10^{3}	1.8246	0.9937
Khan	$q_e = \frac{q_s.b_k.c_e}{\left(1+b_k.c_e\right)^{a_k}}$	q_s	b_k	a_k	R
		58.0900	0.0025	3.5477	0.9935
Radke-Prausnitz	$q_e = \frac{a_{RP}.r_{RP}.c_e}{1+r_{RP}.C_e^{B_{RP}}}$	a_{RP}	r_{RP}	B_{RP}	R
		76.8772	0.0018	1.3917	0.9936
Koble-Corrigan	$q_e = \frac{A.c_e^n}{1+B.C_e^n}$	A	n	B	R
		0.0843	1.2447	0.0095	0.9934
Keller	$q_e = \frac{q_m.a.b.c_e}{\left(1+\left(b.C_e\right)^a\right)^{1/a}}$	q_m	a	b	R
		4.3309	1.8286	0.0167	0.9937
Dobinin-Astakhov	$q_e = q_m.\exp\left(-\left(\frac{RT}{E}\ln\left(1+\frac{1}{c_e}\right)\right)^n\right)$	q_m	E	n	R
		12.2411	44.1117	0.5780	0.9926
Unilan	$q_e = \frac{q_m}{2s}.\ln\left(\frac{1+b.e^s.c_e}{1+b.e^{-s}.c_e}\right)$	q_m	b	s	R
		10.7199	-7.3778×10^{-5}	0.0160	0.9917
Jossens	$c_e = \frac{q_e}{H}.e^{\left(F.q_e^P\right)}$	H	F	P	R
		2.3004×10^{-5}	-10.1635	-0.1302	0.9763
Hill-Debuer	$c_e = \frac{q_e}{b.\left(q_m-q_e\right)}.e^{\left(\frac{q_e}{q_m-q_e}\right)}.e^{\left(\frac{-cq_e}{q_m}\right)}$	q_m	b	c	R
		92.2922	-19.1352	0.0032	0.9863
Frumkin	$c_e = \frac{\theta}{K_{FF}}.\exp\left(\frac{-f.\theta}{1-\theta}\right)$ $\left(\theta = \left(\frac{q_e}{b}\right)\right)$	b	f	k_{FF}	R
		9.8125	-0.3762	1.4021	0.9940
Fowler-Guggenheim	$c_e = \frac{q_e}{k_{FG}.\left(q_m-q_e\right)}.\exp\left(\frac{2.q_e.w}{R.T.q_m}\right)$	q_m	k_{FG}	w	R
		2.4112×10^{4}	8.0759×10^{4}	3.5515×10^{-6}	0.9862
Kiselev	$C_e = \frac{1}{k_1}.\left(\frac{q_e}{q_m-q_e}\right)+\frac{1}{k_1k_n}\left(\frac{q_m}{q_m-q_e}\right)$	k_1	q_m	k_n	R
		0.0639	8.6732	1.2934	0.9905

Table 5. Parameters and correlation coefficients (R) concerning nonlinear three-parameter adsorption isotherms derived from the fitting of experimental data utilizing Curve Expert software for copper adsorption on zeolite modified with SDS

Isotherm	Isotherm equation	SDS-modified natural zeolite			
Reich-Peterson	$q_e = \frac{k_R.c_e}{1+a_R.c_e^g}$	K_R	a_R	g	R
		7.1554×10^{2}	44.0069	0.8074	0.9936
Sips	$q_e = \frac{k_s.a_s.c_e^{B_S}}{1+a_s.c_e^{B_s}}$	K_s	a_S	B_s	R
		24.9633	1.8344	0.5214	0.9882
Hill	$q_e = \frac{q_m.c_e^{n_H}}{K_D+c_e^{n_H}}$	q_m	n_H	K_D	R
		24.9633	0.5214	0.5450	0.9882
Toth	$q_e = \frac{k_T.c_e}{\left(a_T+c_e^z\right)^{\frac{1}{z}}}$	k_T	a_T	Z	R
		32.2852	0.2373	0.3056	0.9895
Khan	$q_e = \frac{q_s.b_k.c_e}{\left(1+b_k.c_e\right)^{a_k}}$	q_s	b_k	a_k	R
		6.2440	92.4183	0.7922	0.9920

Radke-Prausnitz	$q_e = \frac{a_{RP}.r_{RP}.c_e}{1+r_{RP}.C_e^{B_{RP}}}$	a_{RP}	r_{RP}	B_{RP}	R
		16.2598	44.0060	0.8074	0.9915
Koble-Corrigan	$q_e = \frac{A.c_e^n}{1+B.C_e^n}$	A	n	B	R
		45.7995	0.5214	1.8346	0.9882
Keller	$q_e = \frac{q_m.a.b.c_e}{\left(1+\left(b.C_e\right)^a\right)^{1/a}}$	q_m	a	b	R
		105.6347	0.3056	110.5423	0.9895
Dobinin-Astakhov	$q_e = q_m.\exp\left(-\left(\frac{RT}{E}\ln\left(1+\frac{1}{c_e}\right)\right)^n\right)$	q_m	E	n	R
		19.8255	0.3472	1.1541	0.9862
Unilan	$q_e = \frac{q_m}{2s}.\ln\left(\frac{1+b.e^s.c_e}{1+b.e^{-s}.c_e}\right)$	q_m	b	s	R
		50.2683	8.3526	0.0481	0.9906
Jossens	$c_e = \frac{q_e}{H}.e^{\left(F.q_e^P\right)}$	H	F	P	R
		8.5788×10^5	6.1758	0.2082	0.9867
Hill-Debuer	$c_e = \frac{q_e}{b.\left(q_m-q_e\right)}.e^{\left(\frac{q_e}{q_m-q_e}\right)}.e^{\left(\frac{-cq_e}{q_m}\right)}$	q_m	b	c	R
		961.7752	-138.7387	0.1543	0.9816
Frumkin	$c_e = \frac{\theta}{K_{FF}}.\exp\left(\frac{-f.\theta}{1-\theta}\right)$ $\left(\theta = \left(\frac{q_e}{b}\right)\right)$	b	f	k_{FF}	R
		2.3536×10^{-3}	0.5541	-7.7389	0.8911
Fowler-Guggenheim	$c_e = \frac{q_e}{k_{FG}.\left(q_m-q_e\right)}.\exp\left(\frac{2.q_e.w}{R.T.q_m}\right)$	q_m	k_{FG}	w	R
		511.9109	29.8753	2.7846×10^{-3}	0.8206
Kiselev	$C_e = \frac{1}{k_1}.\left(\frac{q_e}{q_m-q_e}\right)+\frac{1}{k_1k_n}\left(\frac{q_m}{q_m-q_e}\right)$	k_1	q_m	k_n	R
		1.7997	24.4968	1.7095×10^8	0.9652

Table 6. Parameters and correlation coefficients (R) of the four-parameter nonlinear adsorption isotherms derived from the fitting of empirical data utilizing Curve Expert software for the adsorption of copper onto unmodified natural zeolite, as well as zeolite modified with CTAB and SDS

Isotherm	**Isotherm equation**	**Unmodified natural zeolite**				
Fritz-Schlunder	$q_e = \frac{c.c_e^\alpha}{1+D.c_e^\beta}$	C	D	α	β	R
		0.4281	0.6950	3.0137	3.4834×10^{-5}	0.9941
Baudu	$q_e = \frac{q_{mB}.b.c_e^{(1+x+y)}}{1+b.c_e^{(1+x)}}$	q_{mB}	b	x	y	R
		0.5986	212.2870	26.8072	0.5863	0.9909
Weber-Van Vliet	$c_e = p_1.q_e^{\left(p_2.q_e^{p_3}+p_4\right)}$	p_1	p_2	p_3	p_4	R
		4.3893	9.0055×10^{-6}	4.5086	1.2825	0.9955
Isotherm	**Isotherm equation**	**CTAB-modified natural zeolite**				
Fritz-Schlunder	$q_e = \frac{c.c_e^\alpha}{1+D.c_e^\beta}$	C	D	α	β	R
		0.1282	1.0335	0.0024	1.3561	0.9936
Baudu	$q_e = \frac{q_{mB}.b.c_e^{(1+x+y)}}{1+b.c_e^{(1+x)}}$	q_{mB}	b	x	y	R
		0.4976	-80.7837	83.0464	0.5615	0.9781
Weber-Van Vliet	$c_e = p_1.q_e^{\left(p_2.q_e^{p_3}+p_4\right)}$	p_1	p_2	p_3	p_4	R
		0.2526×10^2	13.3260	48.6033	5.3003	0.9636
Isotherm	**Isotherm equation**	**SDS-modified natural zeolite**				
Fritz-Schlunder	$q_e = \frac{c.c_e^\alpha}{1+D.c_e^\beta}$	C	D	α	β	R
		4.4239×10^5	2.3908	2.8077×10^4	2.1598	0.9932
Baudu	$q_e = \frac{q_{mB}.b.c_e^{(1+x+y)}}{1+b.c_e^{(1+x)}}$	q_{mB}	b	x	y	R
		2.2958×10^3	6.9355×10^{-3}	-2.0363	1.2444	0.9922
Weber-Van Vliet	$c_e = p_1.q_e^{\left(p_2.q_e^{p_3}+p_4\right)}$	p_1	p_2	p_3	p_4	R
		3.4468×10^{-4}	-3.6159	-1.2620	3.0284	0.9882

The comparison of isotherm fits based on overlap and correlation coefficients for two-, three-, and four-parameter models (Tables 2-6) showed:

For copper adsorption on unmodified natural zeolite:

- Two-parameter models: favorable fits with Volmer, Elovich, Langmuir, and Freundlich isotherms.

- Three-parameter models: Hill-Debuer, Kiselev, Sips, Hill, Koble–Corrigan, Toth, Keller, Dobinin-Astakhov,Radke-prausnitz. Khan, Unilan, Fowler-Guggenheim showed good fits.
- Four-parameter models: Weber-Van Vliet, Fritz-Schlunder, and Baudu isotherms had the best fit.

For copper adsorption on CTAB-modified zeolite:

- Two-parameter models: Jovanovich, Langmuir and Volmer.
- Three-parameter models: Frumkin, Toth, Keller, Reich-peterson, Radke-prausnitz, Khan, Sips, Hill, Koble-Corrigan,Dobinin-Astakhov, Unilan, Kiselev.
- Four-parameter models: Fritz-Schlunder showed highest conformity.

For copper adsorption on SDS-modified zeolite:

- Two-parameter models: Tempkin,Freundlich, Elovich.
- Three-parameter models: Reich-peterson, Khan, Radke-prausnitz, Unilan.
- Four-parameter models: Fritz-Schlunder, and Baudu.

Based on the empirical evidence delineated in this article, a rigorous comparison of adsorption capacity with other scholarly investigations and materials is articulated as follows:

Comparison with natural zeolite in other studies:

- Present Study: The copper adsorption capacity for natural zeolite was documented as 8.98mg/g.
- Oter and Akcay (2007): The adsorption capacity for a Turkish natural zeolite was quantified at 0.173meq/g (approximately equivalent to ~5.5mg/g), which is notably inferior to the value articulated in this study. This variance may be ascribed to the disparate geological origins of the zeolite.
- Dimirkou (2007): Reported a capacity of 13.6mg/g for copper adsorption on natural zeolite, which surpasses the value observed in this investigation.

Comparison with SDS-modified zeolite:

- Present Study: The adsorption capacity of SDS-modified zeolite attained 19.56mg/g
- Harutyunyan et al. (2023): In a scholarly investigation of SDS-modified zeolite, the adsorption capacity for copper ions was ranked fourth subsequent to Co^{2+}, Fe^{2+}, and Ni^{2+}, with multilayer adsorption behavior being documented.
- Clin-Fe Composite: The investigation by Dimirkou (2008) concerning a zeolite-iron oxide composite exhibited an adsorption capacity of 37.5 mg/g, which exceeds that of the SDS-modified zeolite in this study.

Comparison with other modification methods:

- APTES-Modified Zeolite (Shirendev et al., 2022): At an initial copper concentration of 200mg/L, an adsorption capacity of 6.96mg/g was documented, which is significantly lower than the SDS-modified zeolite in this study (19.56mg/g).
- HDTMA-Modified Zeolite (Zekavat et al., 2020): Reported an adsorption capacity of 0.068mmol/g (approximately equivalent to ~4.3mg/g) for copper.
- CTAB-Modified Kaolin (Ma et al., 2016): An adsorption capacity of 38.5mg/g for copper was observed, which is superior to the SDS-modified zeolite in this study.

Comparison with other adsorbents:

- CPC-Modified Zeolite (Bagheri et al., 2024): Documented a capacity of 5.06mg/g for the adsorption of Sunset Yellow dye.

- Zwitterionic Surfactant-Modified Montmorillonite: Demonstrated a lower adsorption capacity for copper in comparison to cationic surfactants.

Comparative summary:

- The SDS-modified zeolite in this study, exhibiting an adsorption capacity of 19.56 mg/g, outperforms numerous zeolites modified through alternative methodologies (*e.g.*, APTES, HDTMA).
- Nevertheless, this capacity is inferior to certain advanced composites (*e.g.*, Clin-Fe) and other modified materials (*e.g.*, CTAB-Kaolin).
- The pronounced efficacy of SDS-modified zeolite in this study corroborates the pivotal role of surface charge and electrostatic interactions in the adsorption mechanism.

This comparative analysis elucidates that while the SDS-modified zeolite in this study demonstrates commendable performance, there exists considerable potential for further enhancement of the adsorption capacity via alternative modification strategies.

In order to examine the mechanism underlying the adsorption of copper ions onto each zeolite variant, the adsorption isotherm that demonstrated the highest correlation coefficient and optimal fit was initially determined for each scenario. Subsequently, the adsorption mechanisms corresponding to all three methodologies were elucidated through a comprehensive analysis of their respective parameters.

3.1. Adsorption mechanism on unmodified zeolite

In the context of copper adsorption onto the unmodified zeolite, the isotherm exhibiting the highest correlation coefficient and optimal fit was identified as the Weber-van Vliet isotherm (R=0.9955) (Table 6). To gain insights into the equilibrium adsorption mechanism and the properties of the adsorbent surface, the equilibrium data were meticulously analyzed employing this specific isotherm. The mathematical representation of this model is articulated in Eq. (3).

$$c_e = p_1.q_e^{\left(p_2.q_e^{p_3}+p_4\right)} \tag{3}$$

The calibrated parameters for this adsorption isotherm are delineated as follows: p_1=4.3893, p_2=9.0055×10^{-6}, p_3=4.5086, and p_4=1.2825. A comprehensive analysis of these parameters elucidates significant insights into the adsorption dynamics exhibited by the system.

The parameter p_4=1.2825, which assumes a function analogous to the exponential coefficient in the Freundlich isotherm model, suggests that the adsorption isotherm curve demonstrates a propensity towards S-shaped behavior within a defined concentration spectrum [58]. This particular isotherm is conventionally observed under conditions where, at lower concentrations, the interactions between the adsorbed molecules and the adsorbent surface are relatively subdued. Conversely, as the initial concentration escalates and the primary adsorption sites become occupied, cooperative interactions among the adsorbed molecules are intensified, culminating in an augmented slope of the adsorption curve [59]. The parameter p_1=4.3893 functions as a scaling coefficient, signifying a moderate level of affinity that the adsorbent has for the target analyte. The magnitude of this parameter implies that a substantially elevated equilibrium concentration within the solution is requisite to attain a specific adsorption capacity.

A particularly notable feature of this model is the inclusion of the corrective term $p_2 \cdot qe^{p_3}$ within the principal exponent. The exceedingly diminutive value of p_2 (approximately 10^{-6}), in conjunction with the considerable value of p_3=4.5086, signifies that this term becomes consequential exclusively at elevated levels of adsorption capacities

(q_e). This behavior can be ascribed to the phenomenon of gradual saturation of the active surface sites. As the adsorbent surface approaches a nearly saturated condition, any additional increase in adsorption capacity necessitates a considerably larger increment in the equilibrium concentration C_e for only a marginal enhancement in q_e. This phenomenon may be attributed to heightened intermolecular repulsions that arise on a densely populated surface and/or the occupation of higher-energy sites, ultimately leaving only lower-energy sites available during the terminal stages of adsorption [60].

In conclusion, it can be inferred that the mechanism of adsorption adheres to a hybrid model:

- At low to moderate concentrations, the behavior of the system is predominantly characterized by a quasi-Freundlich mechanism, which is emblematic of heterogeneous surfaces and may potentially involve cooperative interactions at the inception of the process.
- At elevated concentrations approaching saturation, the pronounced exponential influence emerging from parameter p_3 becomes predominant, effectively encapsulating the phenomena associated with saturation and repulsion among adsorbed molecules.

This analysis substantiates the assertion that the proposed empirical model is adept at quantitatively capturing the kinetic and equilibrium intricacies of the current adsorption system with commendable precision.

3.2. Adsorption mechanism on CTAB-modified zeolite

For the adsorption of copper onto zeolite modified with cetyltrimethylammonium bromide (CTAB), the Frumkin isotherm exhibited the highest correlation coefficient and optimal fit (R=0.9940) as documented in Table 4. In order to elucidate the equilibrium adsorption mechanism and the characteristics inherent to the adsorbent surface, the equilibrium data were subjected to analysis utilizing this isotherm. The mathematical representation for this model is articulated as follows in Eq. (4).

$$c_e = \frac{\theta}{K_{FF}}.\exp\left(\frac{-f.\theta}{1-\theta}\right) \quad \left(\theta = \left(\frac{q_e}{b}\right)\right) \tag{4}$$

The parameters that have been fitted for this isotherm are as follows: K_{FF}=1.4021, b = 9.8125, f = -0.3762. A thorough examination of these parameters yields significant insights into the adsorption behavior. K_{FF} = 1.4021 signifies the adsorption equilibrium constant, suggesting a robust affinity for adsorption. The parameter b =9.8125 indicates a substantial capacity for monolayer adsorption, whereas the parameter f =-0.3762 reflects the presence of weak repulsive interactions. The adsorption of Cu^{2+} ions transpires through a monolayer mechanism characterized by these weak repulsive interactions. The procedural steps involved in the adsorption mechanism encompass:

1) Initial Adsorption: The occupation of energetically favorable active surface sites.
2) Inter-ionic Repulsion: The manifestation of weak repulsive interactions among the charged Cu^{2+} ions.
3) Gradual Saturation: A decline in the adsorption rate as the maximum capacity is approached.

Thermodynamic evaluations reveal that the Gibbs free energy of adsorption $\Delta G°<0$, thereby affirming that the process is spontaneous ($\Delta G° = -RT \ln K_{FF}$). The nature of the adsorption is attributed to physico-chemical interactions, which are regulated by weak repulsion. The surface of the adsorbent is heterogeneous, with adsorption occurring at sites that possess varying energy levels. The Frumkin model effectively describes the isotherm for Cu^{2+} adsorption, illustrating monolayer adsorption accompanied by weak repulsive interactions and a considerable capacity for industrial applications. The current system, characterized by a high adsorption capacity (9.81mg·g^{-1}) and a favorable

adsorption affinity (K=1.402L·mg^{-1}), is optimized for the remediation of industrial wastewater containing copper within the concentration range of 50-200mg·L^{-1}.

3.3. Adsorption mechanism on SDS-modified zeolite

For the process of copper adsorption onto the SDS-modified zeolite, a notably high correlation coefficient and optimal fit were identified for the Redlich-Peterson isotherm (R =0.9936) (Table 5). In order to elucidate the equilibrium adsorption mechanism and the properties of the adsorbent surface, the equilibrium data were meticulously analyzed employing this isotherm. The mathematical representation of this model is articulated by Eq. (5).

$$q_e = \frac{k_R.c_e}{1 + a_R.c_e^g} \tag{5}$$

The fitted parameters pertinent to this isotherm are as follows: k_R =7.1554×10², a_R =44.0069, g =0.8074. An examination of these parameters yields significant insights into the adsorption behavior. The parameter a_R is indicative of the maximum adsorption capacity, the parameter k_R pertains to the equilibrium constant and adsorption affinity, while the parameter g is the exponential parameter that signifies the degree of surface heterogeneity. The values obtained for the model parameters afford a comprehensive understanding of the adsorption mechanism as well as the characteristics of the adsorbent surface. The exceedingly elevated value of parameter a_R indicates an extraordinary adsorption capacity of the examined adsorbent. This elevated value can be ascribed to a remarkably high specific surface area, a porous structure, and a profusion of active adsorption sites present on the adsorbent. Such a high capacity renders this adsorbent exceptionally suitable for practical applications necessitating the removal of substantial quantities of pollutants. The parameter k_R, which denotes adsorption affinity, exhibits a significant value. This finding suggests that the adsorbent possesses a pronounced tendency to engage with the adsorbate molecules, thereby achieving substantial adsorption efficiency even at minimal concentrations. This trait is critical for the remediation of pollutants in low-concentration environments. The value of parameter g, which is marginally less than 1, implies that the adsorption system experiences a slight deviation from ideal behavior and perfectly homogeneous surfaces, as characterized by the Langmuir model. This value corroborates that the adsorbent surface possesses a certain degree of heterogeneity, albeit not to an extreme extent. Such intermediate behavior is frequently observed in real adsorbents that exhibit a distribution of adsorption sites with varying energy levels.

The amalgamation of high capacity (signified by a large a_R value) and robust adsorption affinity (indicated by a large k_R value) positions this adsorbent as a highly effective option for both low and high concentrations of pollutants. In conclusion, the isotherm analysis utilizing the proposed model elucidated that the synthesized adsorbent possesses an exceptionally high capacity and adsorption affinity, with its surface demonstrating partial heterogeneity. These characteristics substantiate the significant potential of this adsorbent for application in diverse treatment processes, ranging from advanced treatment of industrial wastewater to the removal of pollutants from groundwater.

The empirical findings derived from the isotherm fittings exhibit a high degree of concordance with the surface characterization data documented in the academic literature [49]. The notable increase in the adsorption capacity of the SDS-modified zeolite (q_e =19.56mg/g in contrast to 8.98mg/g for the unmodified zeolite) can be directly ascribed to the substantial augmentation in specific surface area (from 19.40 to 72.70m²/g) and mesopore volume (from 1.44 to 3.54cm³/g) [49]. This augmented accessibility of physical sites, in conjunction with the negative surface charge engendered by SDS, which promotes advantageous electrostatic interactions with Cu^{2+} cations, elucidates the

enhanced efficacy of this adsorbent. In contrast, the diminished adsorption capacity noted for the CTAB sample, notwithstanding its elevated surface area, is attributable to the emergence of a positive surface charge that engenders electrostatic repulsion with copper ions. This finding empirically substantiates the assertion that electrostatic interaction constitutes the principal driving force within this system.

4. Conclusion and future perspectives

This study systematically evaluated the effectiveness of natural and surfactant-modified zeolites for copper(II) ion removal from aqueous solutions. The results demonstrated that surface modification of clinoptilolite zeolite with the anionic surfactant sodium dodecyl sulfate (SDS) represents a highly effective strategy for enhancing adsorption capacity. Specifically, the equilibrium adsorption capacity (q_e) of SDS-modified zeolite exceeded that of natural zeolite by more than twofold. In contrast, modification with the cationic surfactant cetyltrimethylammonium bromide (CTAB) proved detrimental, resulting in significantly reduced adsorption performance compared to the unmodified material.

Isotherm analysis revealed that experimental data fitted well to established adsorption models, confirming the monolayer adsorption mechanism for copper(II) ions on natural zeolite surfaces. The comprehensive evaluation of isotherm parameters provided mechanistic insights into the governing surface processes, including cooperative binding interactions at elevated metal concentrations and the progressive saturation of active adsorption sites.

While this investigation successfully elucidated the equilibrium behavior and fundamental adsorption mechanisms, several critical knowledge gaps remain that limit the practical implementation of this technology. Notably, the effects of key operational parameters—including solution pH, adsorbent dosage, contact time, and adsorption kinetics—have not been comprehensively characterized. These limitations pose significant challenges for the design and optimization of full-scale water treatment systems.

To address these research gaps, future investigations should prioritize the systematic optimization of operational parameters through advanced experimental design methodologies, including response surface methodology (RSM) and Design of Experiments (DOE) approaches. Additionally, comprehensive kinetic modeling studies are essential to elucidate the temporal aspects of the adsorption process and mass transfer mechanisms. The implementation of advanced surface characterization techniques, including X-ray photoelectron spectroscopy (XPS), field emission scanning electron microscopy (FESEM), and Brunauer-Emmett-Teller (BET) surface area analysis, will provide definitive validation of the proposed adsorption mechanisms and surface modification effects.

Addressing these research priorities will advance the fundamental understanding of surfactant-modified zeolite systems and facilitate the development of next-generation adsorbent materials with enhanced selectivity, capacity, and operational efficiency for industrial-scale water treatment applications.

Acknowledgement

The authors wish to acknowledge Mr. Reza Fazaeli for his valuable contribution to the analysis of the IR spectra.

Nomenclature

Symbols

R^2	correlation coefficient
ppm	Part Per Million (mg/L)

Abbreviation

CTAB	Cetyltrimethylammonium bromide
SDS	sodium dodecyl sulfate

Sspecific	specific surface area (m2/g)	USEPA	United States Environmental Protection Agency
Sexternal	external surface area (m2/g)	SMZ	surfactant-modified zeolite
Smicro	micropore surface area (m2/g)	VOCs	volatile organic compounds
Vmeso	mesopore volume (cm3/g)	AAS	Atomic Absorption Spectroscopy
Vmicro	micropore volume (cm3/g)	FT-IR	Fourier Transform Infrared
q_e	Quantity of adsorbate per unit mass of adsorbent (mg/g)	SEM	Scanning Electron Microscope
C_0	Initial concentration of the pollutant (mg/L or ppm)	BET	Brunauer-Emmett-Teller
C_e	Equilibrium concentration subsequent to adsorption (mg/L or ppm)	RSM	response surface methodology
V	Volume of solution (L)	DOE	Design of Experiments
m	Mass of adsorbent (g)	XPS	X-ray photoelectron spectroscopy
		FESEM	field emission scanning electron microscopy

References

[1] Briffa, J., Sinagra, E., Blundell, R., 2020. Heavy metal pollution in the environment and their toxicological effects on humans, Heliyon, 6, e04691. http://dx.doi.org/10.1016/j.heliyon.2020.e04691

[2] Ali, H., Khan, E., Ilahi, I., 2019. Environmental chemistry and ecotoxicology of hazardous heavy metals: Environmental persistence, toxicity, and bioaccumulation, Journal of Chemistry, 2019, 6730305. http://dx.doi.org/10.1155/2019/6730305

[3] El-Sherif, I.Y., Tolani, S., Ofosu, K., Mohamed, O.A., Wanekaya, A.K., 2013. Polymeric nanofibers for the removal of Cr(III) from tannery wastewater, Journal of Environmental Management, 129, 410-413. http://dx.doi.org/10.1016/j.jenvman.2013.06.001

[4] Tchounwou, P.B., Yedjou, C.G., Patlolla, A.K., Sutton, D.J., 2012. Heavy metal toxicity and the environment, Experientia Supplementum, 101, 133-164. http://dx.doi.org/10.1007/978-3-7643-8340-4_6

[5] Senila, M., Cadar, O., Senila, L., Hoaghia, A., Miu, I., 2019. Mercury determination in natural zeolites by thermal decomposition atomic absorption spectrometry: Method validation in compliance with requirements for use as dietary supplements, Molecules, 24, 4023. http://dx.doi.org/10.3390/molecules24244023

[6] Rahmany-Samani, A., Ghobadinia, M., Tabatabaei, S.-H., Nourmahnad, N., Danesh-Shahraki, A., 2023. The effect of irrigation and zeolite management on the reduction of cadmium accumulation in rice, Agricultural Water Management, 287, 108448. http://dx.doi.org/10.1016/j.agwat.2023.108448

[7] Kaya, C., Okant, M., Ugurlar, F., Alyemeni, M.N., Ashraf, M., Ahmad, P., 2019. Melatonin-mediated nitric oxide improves tolerance to cadmium toxicity by reducing oxidative stress in wheat plants, Chemosphere, 225, 627-638. http://dx.doi.org/10.1016/j.chemosphere.2019.03.026

[8] Zou, Y., et al., 2016. Environmental remediation and application of nanoscale zero-valent iron and its composites for the removal of heavy metal ions: A review, Environmental Science & Technology, 50, 7290-7304. http://dx.doi.org/10.1021/acs.est.6b00497

[9] Tjandraatmadja, G., et al., 2008. Sources of critical contaminants in domestic wastewater: Contaminant contribution from household products.

[10] Taseidifar, M., Makavipour, F., Pashley, R.M., Rahman, A.F.M.M., 2017. Removal of heavy metal ions from water using ion flotation, Environmental Technology & Innovation, 8, 182-190. http://dx.doi.org/10.1016/j.eti.2017.05.002

[11] García-Niño, W.R., Pedraza-Chaverrí, J., 2014. Protective effect of curcumin against heavy metals-induced liver damage, Food and Chemical Toxicology, 69, 182-201. http://dx.doi.org/10.1016/j.fct.2014.04.019

[12] Borba, C.E., Guirardello, R., Silva, E.A., Veit, M.T., Tavares, C.R.G., 2006. Removal of nickel(II) ions from aqueous solution by biosorption in a fixed bed column: Experimental and theoretical breakthrough curves, Biochemical Engineering Journal, 30, 184-191. http://dx.doi.org/10.1016/j.bej.2006.04.008

[13] Vardhan, K.H., Kumar, P.S., Panda, R.C., 2019. A review on heavy metal pollution, toxicity and remedial measures: Current trends and future perspectives, Journal of Molecular Liquids, 290, 111197. http://dx.doi.org/10.1016/j.molliq.2019.111197

[14] Kim, J.-J., Kim, Y.-S., Kumar, V., 2019. Heavy metal toxicity: An update of chelating therapeutic strategies, Journal of Trace Elements in Medicine and Biology, 54, 226-231. http://dx.doi.org/10.1016/j.jtemb.2019.05.003

[15] Qasem, N.A.A., Mohammed, R.H., Lawal, D.U., 2021. Removal of heavy metal ions from wastewater: A comprehensive and critical review, npj Clean Water, 4, 36. http://dx.doi.org/10.1038/s41545-021-00127-0

[16] Ugwu, E.I., Othmani, A., Nnaji, C.C., 2022. A review on zeolites as cost-effective adsorbents for removal of heavy metals from aqueous environment, International Journal of Environmental Science and Technology, 19, 8061-8084. http://dx.doi.org/10.1007/s13762-021-03560-3

[17] Hedstrom, A., 2001. Ion exchange of ammonium in zeolites: A literature review, Journal of Environmental Engineering, 127, 673-681. http://dx.doi.org/10.1061/(ASCE)0733-9372(2001)127:8(673)

[18] Kesraoui-Ouki, S., Cheeseman, C.R., Perry, R., 1994. Natural zeolite utilization in pollution control: A review of applications to metals effluents, Journal of Chemical Technology & Biotechnology, 59, 121-126. http://dx.doi.org/10.1002/jctb.280590202

[19] Caputo, D., Pepe, F., 2007. Experiments and data processing of ion exchange equilibria involving Italian natural zeolites: A review, Microporous and Mesoporous Materials, 105, 222-231. http://dx.doi.org/10.1016/j.micromeso.2007.04.024

[20] Shi, J., Yang, Z., Dai, H., Lu, X., Peng, L., Tan, X., Shi, L., Fahim, R., 2018. Preparation and application of modified zeolites as adsorbents in wastewater treatment, Water Science and Technology, 77, 621-635. http://dx.doi.org/10.2166/wst.2018.249
[21] Wang, S., Peng, Y., 2010. Natural zeolites as effective adsorbents in water and wastewater treatment, Chemical Engineering Journal, 156, 11-24. http://dx.doi.org/10.1016/j.cej.2009.10.029
[22] Ugwu, E.I., Othmani, A., Nnaji, C.C., 2022. A review on zeolites as cost-effective adsorbents for removal of heavy metals from aqueous environment, International Journal of Environmental Science and Technology, 19, 8061-8084. http://dx.doi.org/10.1007/s13762-021-03560-3
[23] Velarde, L., Nabavi, M.S., Escalera, E., Antti, M.L., Akhtar, F., 2023. Adsorption of heavy metals on natural zeolites: A review, Chemosphere, 328, 138508. http://dx.doi.org/10.1016/j.chemosphere.2023.138508
[24] Irannajad, M., Haghighi, H.K., 2021. Removal of heavy metals from polluted solutions by zeolitic adsorbents: A review, Environmental Processes, 8, 7-35. http://dx.doi.org/10.1007/s40710-020-00476-x
[25] Belviso, C., 2020. Zeolite for potential toxic metal uptake from contaminated soil: A brief review, Processes, 8, 820. http://dx.doi.org/10.3390/pr8070820
[26] Kallo, D., 2001. Applications of natural zeolites in water and wastewater treatment, In: Bish, D.L., Ming, D.W. (Eds.), Natural Zeolites: Occurrence, Properties, Applications, Mineralogical Society of America, Washington, DC, pp. 519-550.
[27] Bish, D.L., Ming, D.W., 2001. Applications of natural zeolites in water and wastewater treatment, In: Natural Zeolites: Occurrence, Properties, Applications, Mineralogical Society of America, Washington, DC, pp. 519-550.
[28] Krstić, V., 2021. Role of zeolite adsorbent in water treatment, In: Handbook of Nanomaterials for Wastewater Treatment, Elsevier, Amsterdam, pp. 417-481.
[29] Bouffard, S.C., Duff, S.J.B., 2000. Uptake of dehydroabietic acid using organically tailored zeolites, Water Research, 34, 2469-2476. http://dx.doi.org/10.1016/S0043-1354(99)00385-4
[30] Sullivan, E.J., Carey, J.W., Bowman, R.S., 1998. Thermodynamics of cationic surfactant sorption onto natural clinoptilolite, Journal of Colloid and Interface Science, 206, 369-380. http://dx.doi.org/10.1006/jcis.1998.5703
[31] Karadag, D., Akgul, E., Tok, S., Erturk, F., Kaya, M.A., Turan, M., 2007. Basic and reactive dye removal using natural and modified zeolites, Journal of Chemical & Engineering Data, 52, 2436-2441. http://dx.doi.org/10.1021/je700392e
[32] Karadag, D., Turan, M., Akgul, E., Tok, S., Faki, A., 2007. Adsorption equilibrium and kinetics of reactive black 5 and reactive red 239 in aqueous solution onto surfactant-modified zeolite, Journal of Chemical & Engineering Data, 52, 1615-1620. http://dx.doi.org/10.1021/je700107n
[33] Benkli, Y.E., Can, M.F., Turan, M., Celik, M.S., 2005. Modification of organo-zeolite surface for the removal of reactive azo dyes in fixed-bed reactors, Water Research, 39, 487-493. http://dx.doi.org/10.1016/j.watres.2004.10.008
[34] Bowman, R.S., 2003. Applications of surfactant-modified zeolites to environmental remediation, Microporous and Mesoporous Materials, 61, 43-56. http://dx.doi.org/10.1016/S1387-1811(03)00354-8
[35] Cortes-Martinez, R., Martinez-Miranda, V., Solache-Rios, M., Garcia-Sosa, I., 2004. Evaluation of natural and surfactant-modified zeolites in the removal of cadmium from aqueous solutions, Separation Science and Technology, 39, 2711-2730. http://dx.doi.org/10.1081/SS-200026784
[36] Cortes-Martinez, R., Solache-Rios, M., Martinez-Miranda, V., Alfaro-Cuevas, R., 2007. Sorption behavior of 4-chlorophenol from aqueous solutions by a surfactant-modified Mexican zeolitic rock in batch and fixed bed systems, Water, Air, and Soil Pollution, 183, 85-94. http://dx.doi.org/10.1007/s11270-006-9319-3
[37] Haggerty, G.M., Bowman, R.S., 1994. Sorption of chromate and other inorganic anions by organo-zeolite, Environmental Science & Technology, 28, 452-458. http://dx.doi.org/10.1021/es00052a015
[38] Kuleyin, A., 2007. Removal of phenol and 4-chlorophenol by surfactant-modified natural zeolite, Journal of Hazardous Materials, 144, 307-315. http://dx.doi.org/10.1016/j.jhazmat.2006.10.036
[39] Dakovic, A., Tomasevic-Canovic, M., Rottinghaus, G., Dondur, V., Masic, Z., 2003. Adsorption of ochratoxin A on octadecyldimethyl benzyl ammonium exchanged-clinoptilolite-heulandite tuff, Colloids and Surfaces B: Biointerfaces, 30, 157-165. http://dx.doi.org/10.1016/S0927-7765(03)00070-1
[40] Dakovic, A., Tomasevic-Canovic, M., Rottinghaus, G.E., Matijasevic, S., Sekulic, Z., 2007. Fumonisin B-1 adsorption to octadecyldimethylbenzyl ammonium-modified clinoptilolite-rich zeolitic tuff, Microporous and Mesoporous Materials, 105, 285-290. http://dx.doi.org/10.1016/j.micromeso.2007.03.029
[41] Dakovic, A., Matijasevic, S., Rottinghaus, G.E., Dondur, V., Pietrass, T., Clewett, C.F.M., 2007. Adsorption of zearalenone by organomodified natural zeolitic tuff, Journal of Colloid and Interface Science, 311, 8-13. http://dx.doi.org/10.1016/j.jcis.2007.02.033
[42] Ghiaci, M., Abbaspur, A., Kia, R., Seyedeyn-Azad, F., 2004. Equilibrium isotherm studies for the sorption of benzene, toluene, and phenol onto organo-zeolites and as-synthesized MCM-41, Separation and Purification Technology, 40, 217-229. http://dx.doi.org/10.1016/j.seppur.2004.03.003
[43] Lemic, J., Tomasevic-Canovic, M., Adamovic, M., Kovacevic, D., Milicevic, S., 2007. Competitive adsorption of polycyclic aromatic hydrocarbons on organo-zeolites, Microporous and Mesoporous Materials, 105, 317-323. http://dx.doi.org/10.1016/j.micromeso.2007.04.003
[44] Lemic, J., Kovacevic, D., Tomasevic-Canovic, M., Kovacevic, D., Stanic, T., Pfend, R., 2006. Removal of atrazine, lindane and diazinone from water by organo-zeolites, Water Research, 40, 1079-1085. http://dx.doi.org/10.1016/j.watres.2006.01.008
[45] Noroozifar, M., Khorasani-Motlagh, M., Abbaspur, A., 2005. Sorption of phenol from aqueous solutions by cetylpyridinium modified natural zeolite, Journal of Hazardous Materials, 124, 211-216. http://dx.doi.org/10.1016/j.jhazmat.2005.05.002
[46] Misaelides, P., Zamboulis, D., Sarridis, P., Warchol, J., Godelitsas, A., 2008. Chromium(VI) uptake by polyhexamethylene-guanidine-modified natural zeolitic materials, Microporous and Mesoporous Materials, 108, 162-167. http://dx.doi.org/10.1016/j.micromeso.2007.03.038

[47] Bagheri, A., Khabbaz, S.H., Rafati, A.A., 2024. Comparison of the natural and surfactant-modified zeolites in the adsorption efficiency of sunset yellow food dye from aqueous solutions, Scientific Reports, 14, 22511. http://dx.doi.org/10.1038/s41598-024-72515-8
[48] Ma, L., Chen, Q., Zhu, J., Xi, Y., He, H., Zhu, R., Tao, Q., Ayoko, G.A., 2016. Adsorption of phenol and Cu(II) onto cationic and zwitterionic surfactant modified montmorillonite in single and binary systems, Chemical Engineering Journal, 283, 880-888. http://dx.doi.org/10.1016/j.cej.2015.08.009
[49] Harutyunyan, L.R., Tangamyan, L.S., Manukyan, A.V., Harutyunyan, R.S., 2023. Characterization of both anionic and cationic surfactant-modified natural zeolite and its application for removal of metal-ions from aqueous medium, Voprosy Khimii i Khimicheskoi Tekhnologii, (2), 31-40. http://dx.doi.org/10.32434/0321-4095-2023-147-2-31-40
[50] Majidi Trojeni, M., Samadi-Maybodi, A., Shafiei, H., 2025. Investigating the adsorption of volatile organic compounds from kerosene using clinoptilolite (natural zeolite) modified by cationic surfactant cetyltrimethylammonium bromide, MethodsX, 14, 103354. http://dx.doi.org/10.1016/j.mex.2025.103354
[51] Shirendev, N., Bat-Amgalan, M., Kano, N., Kim, H.-J., Gunchin, B., Ganbat, B., Yunden, G., 2022. A Natural Zeolite Developed with 3-Aminopropyltriethoxysilane and Adsorption of Cu(II) from Aqueous Media, Applied Sciences, 12, 11344. http://dx.doi.org/10.3390/app122211344
[52] Zekavat, S.R., Raouf, F., Talesh, S.S.A., 2020. Simultaneous adsorption of Cu2+ and Cr (VI) using HDTMA-modified zeolite: isotherm, kinetic, mechanism, and thermodynamic studies, Water Science and Technology, 82, 1808–1824. http://dx.doi.org/10.2166/wst.2020.448
[53] Oter, O., Akcay, H., 2007. Use of natural clinoptilolite to improve water quality: Sorption and selectivity studies of lead(II), copper(II), zinc(II), and nickel(II), Water Environment Research, 79, 329-335. http://dx.doi.org/10.2175/106143007X172633
[54] Doula, M.K., 2006. Removal of Mn^{2+} ions from drinking water by using clinoptilolite and a clinoptilolite-Fe oxide system, Water Research, 40, 3167-3176. http://dx.doi.org/10.1016/j.watres.2006.06.021
[55] Dimirkou, A., 2007. Uptake of Zn^{2+} ions by a fully iron-exchanged clinoptilolite: Case study of heavily contaminated drinking water samples, Water Research, 41, 2763-2773. http://dx.doi.org/10.1016/j.watres.2007.04.003
[56] Dimirkou, A., Doula, M.K., 2008. Use of clinoptilolite and an Fe-overexchanged clinoptilolite in Zn^{2+} and Mn^{2+} removal from drinking water, Desalination, 224, 280-292. http://dx.doi.org/10.1016/j.desal.2007.08.004
[57] Saadi, R., Saadi, Z., Fazaeli, R., Fard, N.E., 2015. Monolayer and multilayer adsorption isotherm models for sorption from aqueous media, Korean Journal of Chemical Engineering, 32, 787-799. http://dx.doi.org/10.1007/s11814-015-0045-z
[58] Foo, K.Y., Hameed, B.H., 2010. Insights into the modeling of adsorption isotherm systems, Chemical Engineering Journal, 156, 2-10. http://dx.doi.org/10.1016/j.cej.2009.09.013
[59] Lim, L.B.L., Priyantha, N., Hei, C.W., Zehra, T., Then, C.W., 2015. Comprehensive study on adsorption behavior and mechanism of methylene blue by activated carbon derived from Enteromorpha prolifera, Arabian Journal of Chemistry, 13, 3031-3044. http://dx.doi.org/10.1016/j.arabjc.2018.08.009
[60] Wang, J., Guo, X., 2020. Adsorption isotherm models: Classification, physical meaning, and application, Journal of Environmental Chemical Engineering, 8, 104261. http://dx.doi.org/10.1016/j.jece.2020.104261